International Journal of Engineering Trends and Technology
ISSN: 2231–5381 / https://doi.org/10.14445/22315381/IJETT-V73I8P106

Volume 73 Issue 8, 73-90, August 2025

Original Article

Performance Optimization of a Cone Enhanced Split Reaction Turbine by Response Surface Methodology

Alberto E. Lastimado Jr[1,2]*, Wilvin O. Siasico[2], Janiel D. Posada[2], Julius Cydrick E. Alvaro[2], Philip Arnold Q. Baes[2], Jay Ar C. Cuerbo[2], Mark Ryan R. Raneses[2], Stevenson F. Diolas[2], Hamza M. Amer[2], Ryan P. Nassef[2], May Y. Sodicta[2], Moammar A. Abdulnasser[2], Jann Clyde M. Nalla[2], Abdul Jabber S. Domado[2], Jalal Bazeron[2]

[1]*Engineering Department, North Eastern Mindanao State University - Bislig Campus, Surigao del Sur, Philippines.*
[2]*Department of Mechanical Engineering, Mindanao State University-Marawi, Marawi City, Philippines.*

[*]*Corresponding Author : alastimado@nemsu.edu.ph*

Received: 25 March 2025 Revised: 17 July 2025 Accepted: 22 July 2025 Published: 30 August 2025

Abstract - *This study investigates the relationship between water flow rate and the efficiency of a Cone-Enhanced Split Reaction Turbine (CESRT), which is typically used in pico-hydro systems for low-head hydropower applications. The research uses a Response Surface Methodology (RSM) to analyze the impact of cone size, torque, and bypass angle on turbine performance. The experimental setup simulates a pico-hydro system, allowing for controlled manipulation of flow rate and measurement of turbine performance. A cone-enhanced split reaction turbine is tested with varying cone size heights, and data is collected on torque, flow rate, and speed under different load resistances and bypass angle settings. The results show that cone size significantly impacts volume flow rate, with the 2.25-inch cone providing the most efficient performance. Increasing both torque and bypass angle generally leads to a higher volume flow rate, but the magnitude of this effect varies depending on the cone size. The bypass angle also plays a significant role in the flow dynamics, particularly for larger cone sizes, while torque has minimal impact on volume flow rate across all cone configurations. The optimum volume flow rate and efficiency conditions are achieved at a torque of 60 N-m, a bypass angle of 22.5°, and a 2.25-inch cone turbine type. Under these conditions, the maximum achieved volume flow rate is 79.7799 m³/hr, and the turbine's efficiency is 77.0772%. The study concludes that the RSM model is valid for predicting the volume flow rate of the cone-enhanced split reaction turbine and can be used to optimize its design and operation.*

Keywords - *Cone enhanced split reaction turbine, Energy conversion, Pico-hydropower, Response surface methodology, Split reaction turbine.*

1. Introduction

The increasing global energy needs, fueled by economic growth and population increase, along with the urgent need to combat climate change, has strengthened the search for renewable, sustainable energy sources [1]. Pico-hydropower plays a major role in delivering sustainable power solutions, especially for off-grid communities within developing nations that are unreachable by electricity grids [2, 3]. It creates something less than 5 kW of power generation. Because of these systems' offering a localized power source and influence on local water resources, they have relatively little environmental impact compared to large-scale hydro projects. Advancing local economic development is advantageous, along with upgraded energy security and living standards. However, pico-hydropower development faces certain problems, such as high initial costs, a need for site-specific designs, potential water flow variability resulting from seasonal or weather effects, and technical skills to manufacture, install, and maintain. In order to ensure long-term sustainability and economic robustness of pico-hydro installations, the turbines must be efficient, strong, and locally manufacturable [4]. They must also adapt to diverse operating conditions if sites have a low head.

The Split Reaction Turbine (SRT), which is also known as a split-type pure reaction turbine, represents a most promising technology for pico-hydropower applications because it shows a particular suitability for low-head hydro resources. Its design is of a fundamentally simple nature, consisting of a rotating nozzle that bifurcates the water flow into two streams. Rotational force is generated this way as these streams exit through curved blades [2, 5]. This intrinsic simplicity translates to lower manufacturing costs along with easier maintenance, which critically advantages deployment in resource-limited settings. Pioneering work by [5-7] demonstrated the potential of SRTs for low-head (and ultra-low head) applications, achieving efficiencies in the 65-70% range. Their research highlighted the turbine's straightforward

manufacturing process and its capability to convert hydro energy effectively under such conditions. Furthermore, their work underscored the straightforward manufacturing processes associated with SRTs, often involving the modification of readily available materials such as PVC pipes, and confirmed their capacity to convert hydraulic energy under such challenging head conditions effectively. Date and his collaborators systematically investigated the influence of key parameters, including operating head, water flow rate, and nozzle diameter, on SRT performance.

Despite the progress in understanding SRTs, significant research gaps persist in optimizing their design and operation, particularly for pico-hydropower systems. There is a demonstrably limited understanding of how specific internal geometric modifications influence hydraulic efficiency. For example, the effects of different cone sizes or turbine heights on performance within the SRT structure remain largely uninvestigated because most studies consider overall design instead of these precise factors [1]. An important knowledge gap remains while maximizing SRT efficiency due to the lack of detailed investigation into internal flow modifiers. Furthermore, few experimental studies examine the detailed relationships of water flow rate, detailed turbine geometry, coupled with overall efficiency in the context of [1, 4], which are thorough and controlled. Strong optimization needs detailed parametric analysis for success. This analysis is missing from much existing work. Also compounding this is the more limited comparative analysis of SRT efficiency across different configurations and operating conditions, which obstructs the development of more generalized design guidelines for various applications.

This study introduces a novel design modification to address these identified limitations: the Cone-Enhanced Split Reaction Turbine (CESRT). This innovation involves the incorporation of a strategically designed cone-shaped insert within the conventional SRT structure. The primary hypothesis is that this cone will optimize turbine performance by directing and concentrating the water flow towards the turbine's exit nozzles, thereby significantly altering the internal flow dynamics for improved momentum transfer and reduced hydraulic losses. The novelty of the present work lies not only in proposing the CESRT design but, more critically, in the systematic experimental investigation and optimization of this design through varying cone sizes in conjunction with operational parameters like torque and bypass angle, utilizing a rigorous statistical methodology. This approach moves beyond ad-hoc design modifications to a data-driven process for identifying optimal configurations. This methodological rigor is a key contribution of this research when compared to previous SRT studies that often focused on broader design aspects or lacked detailed parametric optimization.

Therefore, this research's primary objective is to conduct a comprehensive investigation into optimizing the Cone-Enhanced Split Reaction Turbine (CESRT). This involves systematically analyzing the effects of varying cone sizes, applied torque, and bypass valve angles on the turbine's volumetric flow rate and overall efficiency. To achieve this, the study uses Response Surface Methodology (RSM) to explore the complex design space well, find the best parameter settings, and make strong predictive models for turbine performance, mainly using a Central Composite Design (CCD). The findings from this study should help develop much more efficient, cost-effective, and strong pico-hydropower systems. The systems' deployment in remote regions will ease sustainable energy conversion and increase energy access.

2. Literature Review

2.1. Development of Simple Split Reaction Turbine Design

The Split Reaction Turbine (SRT), also known as a split-type pure reaction turbine, is now an impressive technology regarding pico-hydropower systems since it offers a specific opportunity with low-head hydro resources [2]. Off-grid communities benefit from pico-hydropower's sustainable energy source. It generates power at less than 5 kW, most especially in the developing nations. Simplicity characterizes an SRT's fundamental design, typically with a rotating nozzle assembly dividing incoming water flow into two streams. These streams are then discharged through curved passages or blades, generating rotational force from the reaction principle [6, 7, 2]. Due to its core design, this ease benefits users so much. Manufacturing costs go down because maintenance is simpler, so deployment is easier in resource-poor areas. SRTs are suited to apply for low-head applications, which are defined by hydraulic heads from 0.5 to 3 meters, which are sometimes termed "ultra-low-head," and they expand access to renewable energy.

SRTs operate on reaction principles because rotational force is generated as water thrusts from nozzles. The split flow layout is a main feature. [5-7] established this fact indeed. SRTs are able to achieve efficiencies in the range of 65-70% under conditions from low to ultra-low head. For example, an SRT with a 0.122 m rotor diameter produced 150 Watts of electrical power at 40 kPa with a water flow rate of about 20 L/sec [5-7]. Theoretical investigations do also suggest that simple reaction turbines, including SRTs, tend to perform better at higher rotational speeds, as this implies smaller rotor diameters for a constant head.

The development of the SRT can be contextualized in that simple reaction turbine designs are continuing to evolve. The SRT itself emerged from an improvement of the Cross Pipe Turbine (CPT) [4, 8]. Because of constituent components' fixed dimensions, the CPT, often constructed out of standard pipe fittings, met limits throughout, achieving adaptable nozzle exit areas with smaller rotor sizes. As a consequence, CPTs did generally exhibit lower efficiencies, and some of the reports indicated the values were around 53%. The Z-Blade

turbine, introduced by [2, 4, 8, 9] more recently in 2014, represents a further advancement in this lineage. Standard PVC fittings plus easily modifiable nozzles are used by the Z-Blade turbine; it aims for maximum simplicity in design and fabrication while achieving high efficiencies, reportedly up to 78-82% under specific head conditions. In comparison to CPTs and to earlier SRT configurations, this design offers distinct advantages with regard to cost and manufacturing ease. The designs of simple reaction turbines experienced gradual improvement. CPT progressed to SRT, and the Z-Blade turbine depicted that progression. Later designs try to address shortcomings of predecessors with a continued focus. The focus is based upon manufacturability with cost-effectiveness plus performance, especially for pico-hydropower's low-head and low-flow conditions.

2.2. Flow Dynamics Modification

Various strategies have been explored that do involve modifications of the internal geometry within turbines. Guide vanes are common in Francis turbines [10], which are reaction turbines. Pumps as turbines or PATs also employ them in the interior [11]. They function to optimally direct the incoming flow onto the runner blades, improving overall efficiency as they control flow rate and operational stability. Cone-shaped elements and diffusers represent internal flow modifiers, too. Water flow accelerates to the blades through a cone at a rotor inlet. This acceleration with streamlining is particularly obvious in propeller-type micro-hydraulic turbines. Consequently, the torque exerted on the runner can increase, leading to improved power generation efficiency. One study focusing on a self-powered IoT turbine flowmeter determined that a cone whose diameter equals 0.375 times the blade outer diameter (d=0.375D) maximized power efficiency because it produced a 1.12-fold increase versus a rotor lacking a cone [12]. The cone induced an increase in the pressure differential across all the blades. This improved the system. The angle for the cone also has an influence on performance in mixed inflow turbines because researchers identified it as a more important parameter, and engineers employ conical diffusers to recover pressure and manage flow separation downstream from the runner. To successfully apply such internal flow modifiers in diverse turbine types presents a compelling precedent when investigating their possible benefits inside SRTs. The efficacy of these modifications is intrinsically linked with the specific turbine geometry and the prevailing flow regime. Research on vertical axis wind turbines (VAWTs) has also explored inverted cone structures, and the cone angle influences the power coefficient and operational torque fluctuations [13, 14]. Such internal flow modifiers have been successfully applied within diverse turbine types, acting as a compelling precedent.

Their possible benefits within SRTs should thus be under investigation. Yet, one must realize that the effectiveness of such changes naturally connects to the turbine's exact shape and flow state, so a systematic study is needed for SRTs, a field that experts have so far neglected.

2.3. Turbine Design Optimization Methodologies

The hydro turbine's design and optimization are intrinsically detailed tasks because many geometric and operational parameters are interrelated [15]. Consequently, various optimization techniques have been employed, coupled with these techniques that range from classical theoretical analyses to iterative experimental approaches toward more advanced computational and statistical methodologies [16]. RSM has come about as a strong statistical tool for the modeling as well as the optimizing of designs and processes in which several independent variables do influence a response of interest [9]. RSM's main strength lies in efficiently probing the design space, finding key links between factors, and defining ideal parameter values using far fewer experimental runs than typical single-factor methods [17]. In cases when physical experiments or computationally intensive simulations are actually the topic, then this efficiency is definitely important.

RSM has been applied with success for hydro turbine type optimization. This array of turbines is beyond simple. For instance, within the context of Gorlov helical turbines, RSM has been used to optimize parameters such as the number of blades, helix angle, and aspect ratio so that the power coefficient (CP) is maximized and optimal CP values around 0.3072 are achieved [17]. Likewise, for Archimedes screw turbines, RSM simplified the optimization of variables like flow rate, inclination angle, pitch, diameter, and number of blades, thus causing important gains in efficiency [18] and power output [19, 20]. Researchers also used RSM to optimize propeller hydrokinetic turbines to find the best number of blades plus hub-to-tip diameter ratio, which gave maximal CP values (e.g., 53.62%). Beyond pico and small-scale turbines, RSM has been applied to optimize energy in larger hydropower plants, such as the Jebba hydropower plant. This generates it by identifying optimal discharge ranges and pressure drop optimize turbines in free vortex systems [21]. Its selection is greatly validated through RSM's common and successful deployment all across these varied hydro turbine applications as a truly appropriate strong methodology for turbomachinery, which is a quite complex optimization task.

RSM is typically applies by developing regression models, often second-order polynomial equations, based on data that experiments obtain. These models predict turbine performance metrics like efficiency, power coefficient, and flow rate. The metrics act as parameters for the investigated design [9]. The statistical importance of the model and individual factors with their interactions is assessed through Analysis Of Variance (ANOVA). For turbine systems, the ability of RSM to elucidate interactions between those parameters is particularly valuable. The effect of one design choice can be contingent upon another's level in these systems. A thorough understanding helps you achieve true system optimization. Do not rely upon single-parameter adjustments because they could mislead you. RSM is known as a

prominent technique for hydro turbine design. Also, other optimization approaches such as genetic algorithms (GA) and various metaheuristic methods are used [17, 18, 22].

3. Materials and Methods

3.1. Specification on Turbine Cone Size of CESRT

The specifications for the CESRT design and its cone component are illustrated in Figure 1. In Figure 1(a), adopted from [6], the turbine's cylindrical section is illustrated, including its height (h=8.0 in), diameter (d=7.5 in), and thickness (t=0.50 in) of the base board. The turbine cone is highlighted in Figure 1(b) by its varying heights (0.0 in, 2.25 in, 2.5 in, 2.75 in, 3.0 in, 3.25 in) and radius (r=3.75 in). The assembled turbine with the cone inserted is depicted in Figure 1(c), which indicates the cone's size variations in relation to the turbine's overall dimensions. These cones are removable and made from wood (mahogany tree). The CESRT is manufactured by splitting a PVC pipe in half and attaching the halves to the top and bottom plates to create the exit nozzles. This simple design allows the turbine to be manufactured without specialized skills or costly materials. The split pipe design was inspired by the Savonius wind rotor [5-7]. The manufacturing process involves splitting a plastic pipe, drilling the pipe sections for screws, drilling the top and bottom cover plates for screws and the flange coupling, and creating an orifice in the bottom plate for water intake and the rotary seal. Plastic is used for the pipe and covers because it is corrosion-resistant, requires little to no balancing due to the symmetry, and is simple to assemble.

3.2. Experimental Setup and Procedure

A closed-loop system designed to evaluate the performance of the CESRT. Two pumps provided the necessary water flow, circulating it through the piping. A ball valve for the bypass angle, strategically placed within the piping, allowed for precise water flow rate control. An electrodynamometer was integrated into the setup to quantify the turbine's torque and power. Finally, a water tank served as the reservoir and turbine house where the CESRT was placed, completing the closed-loop system. The experiment aimed to analyze the performance of the CESRT under varying operational conditions. To achieve this, a controlled environment was established using two Robin EY20D 5hp engine pumps (Model SCR-80R), providing a consistent water flow. Precise measurements were obtained using a handheld ultrasonic flow meter (TUF-2000H) for flow rate, a piezometer for pressure head, a digital tachometer (DT-2234B) for turbine speed, and an electrodynamometer (Lab-Volt 8960) for torque. The experiment began by filling the water drum to a level that ensured proper turbine operation. The turbine was tested with an internal cone of varying cone size heights, secured using flanges and fasteners. Initially, the net head was determined with full pump capacity, no load, and no turbine, resulting in a measurement of 1.50 meters. Subsequently, each turbine was subjected to tests involving varying load resistances with 20-second intervals between adjustments for flow stabilization. Torque, volume flow rate, and speed were recorded at each load setting. Following this, the ball valve was adjusted to distinct positions (bypass angle), allowing 80 seconds for stabilization at each position, and the same parameters were measured. This process was repeated for each cone size height by the test runs suggested by CCD of RSM [23]. All data were recorded in a structured format, and subsequent data analysis was employed to evaluate the CESRT performance.

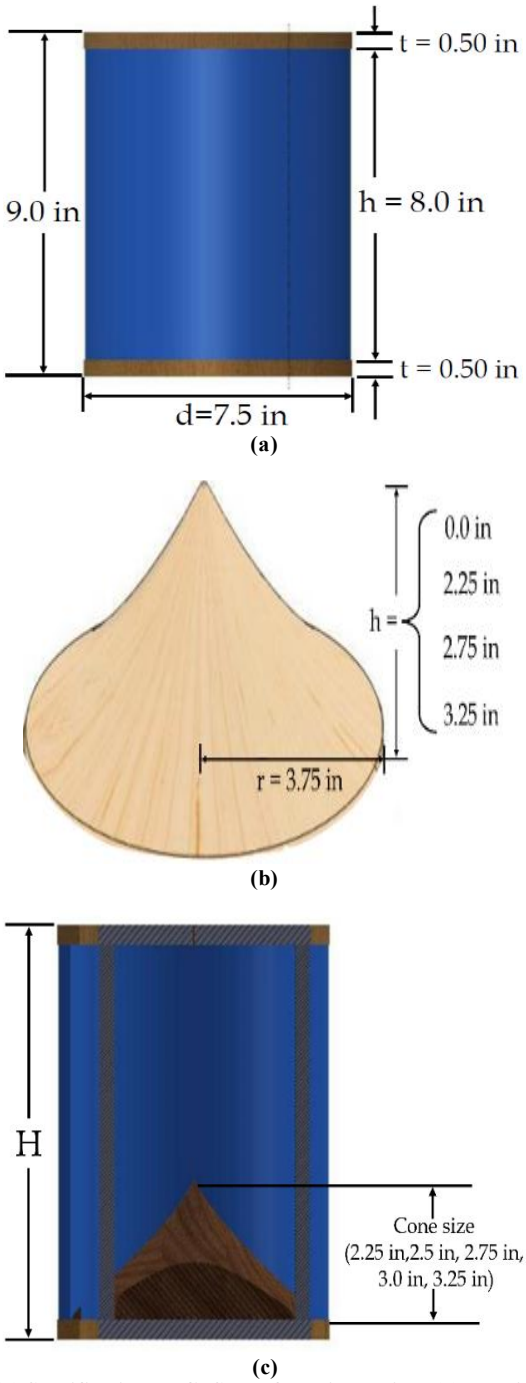

Fig. 1 (a) Specification on CESRT of turbine design, (b) Turbine cone size, and (c) Installation of cone set-up.

The power input, power output and efficiency were calculated using Equations 1, 2 and 3 [24-26]:

$$P_{input} = \rho \cdot g \cdot Q \cdot H \quad (1)$$

$$P_{output} = \frac{2\pi TN}{60} \quad (2)$$

$$n_t = \frac{P_{output}}{P_{input}} x\ 100\% \quad (3)$$

Where ρ represents the density (kg/m^3), g the gravitational acceleration due to gravity (m/s^2), Q the volume flow rate (m^3/s), H is the head, T is the torque (N-m), N is the speed (rpm), and n_t The turbine efficiency.

3.3. Design of Experiment

The study used Response Surface Methodology (RSM) to analyze how different cone sizes affected our experiment. The RSM is a way to build a mathematical model from our experimental data. It helps us figure out the best settings for our variables with the fewest experiments possible and shows us how they interact [21]. The process of using RSM for optimization can be broken down into six main steps [27]:

(1) By establishing the experiment's limits, we are choosing variables independent of the experiment but with notable influences on it.
(2) Arrange the experiment design and run the tests in accordance with it.
(3) Statistical-mathematical analysis of acquired experimental data via an appropriate solution of a polynomial function.
(4) Model fit evaluation, including graphs, p-values, R^2, etc.
(5) Verification of need and possibility for a move toward the intended area (should one side of the range be optimal)
(6) Get optimal values for every variable.

This study utilized a statistical experiment design with three independent variables to investigate their effect on the response variable. Two variables were numerical: torque (A, measured in m/s) and bypass angle (B, measured in degrees). The third variable was categorical: turbine cone size types (C). Each factor's specific ranges and levels were determined according to Equation 4 of the experimental design.

$$Y = f(X_1, X_2 \ldots . X_n) \quad (4)$$

The experiment intended to optimize the response variable Volume Flow Rate (Y) by relating it to independent variables (X_n). Under the best conditions, a Central Composite Design (CCD) improved the volume flow rate. They did conduct the experiment arbitrarily so as to minimize errors as well as influence from unbounded factors. The statistical parameters were computed using the Analysis of Variance (ANOVA). To model the response relationship with independent variables, response surface methods were applied. The total number related to experimental runs labeled "(N)" was found through using Equation 5 [11-13] so as to assess the impact of one categorical factor plus two numerical factors.

$$N = n_t(2^n + 2n + n_c)$$
$$N = 4x(2^2 + 2\,x2 + 3) = 44 \quad (5)$$

Where N represents the total number of runs, n_t Denotes the quantity of categorical factors, n represents the number of numerical factors, and n_c Is the number of replications.

3.4. Data Analysis

Mathematical analysis plays a critical role in validating the practical applicability of theoretical models. By comparing the variations caused by deliberate changes in variables with the inherent, random errors in the data, researchers can discern whether a model accurately reflects real-world phenomena. This process is often facilitated by the use of ANOVA, which effectively separates the impact of controlled variables from the influence of chance [23]. This approach ensures that models are not merely mathematical constructs but reliable tools for understanding and predicting outcomes in practical domains, bridging the gap between theory and application. Design-Expert 12.0 software from Stat-Ease 360® to meticulously analyze experimental data and construct a predictive model, employing a one-way ANOVA to determine the significance of each variable's influence. This statistical methodology enabled them to evaluate the model's adequacy and fitness, ensuring it accurately represented the relationship between variables and responses. A p-value below 0.05 was used as a threshold for significance, indicating that observed effects were unlikely due to random chance. Model validation was then carried out by calculating the coefficient of determination (R^2), supported by the F-value to confirm its statistical significance. A lack-of-fit test was conducted to ensure the model's robustness further, and it differentiated between residual and pure errors at replicated points [14, 16]. PRESS was finally used as an index to assess the model's predictive capability. This adhered to established methodologies from previous studies and lent further credence to all of the findings.

4. Results and Discussion

4.1. CFD Analysis of CESRT with a Split Angle of 0°

Figure 2 depicts the fundamental principle of action and reaction in fluid dynamics through a simplified linear jet scenario, which lays the groundwork for understanding more complex systems. A pipe with a zero-degree inner split angle expels a liquid jet with velocity (V_o), impacting an obstruction. This impact generates a force (F_n) normal to the split edge, equivalent to the force in the x-direction due to the horizontal jet. Simultaneously, the pipe experiences an equal and opposite reaction force (F_R), illustrated in the inset. This implies a shift from the simple linear force to a rotational system, such as a turbine. In such a system, the fluid's velocity

would have a tangential component, leading to a rotational force or torque. This rotational force is crucial for driving turbines, where the momentum of the fluid is converted into rotational motion.

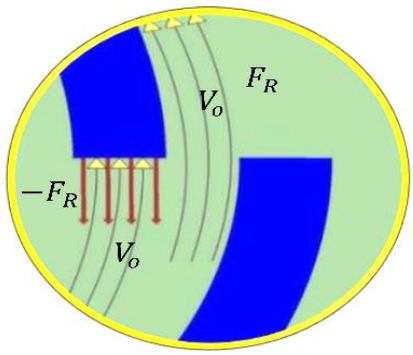

Fig. 2 Impact of the Jet on the turbine inner split edge

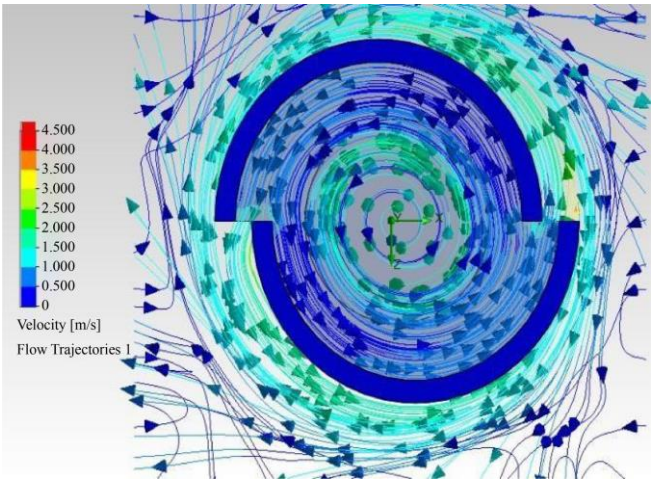

Fig. 3 Simulation of velocity flow trajectories of water in a turbine with a split edge angle 0°

Figure 3 represents the turbine's computational fluid dynamics (CFD) simulation with a split edge angle of 0°. The region reveals a well-defined flow pattern, indicative of efficient fluid distribution. The velocity vectors and flow trajectories demonstrate that the incoming fluid stream is effectively divided into two symmetrical outflow paths with minimal lateral deviation. This observation confirms the design's capability to achieve a precise split without inducing significant turbulence or recirculation. The color-coded velocity magnitude scale, ranging from 0 to 4.5 m/s, indicates a relatively uniform velocity distribution across the exit region. This uniformity suggests a low-pressure drop and reduced energy losses, which are critical factors in optimizing the device's overall efficiency. Furthermore, the absence of abrupt changes in flow direction or velocity gradients suggests that the design minimizes the potential for cavitation or erosion, enhancing the device's long-term reliability.

The fundamental role of splitter blades in turbomachinery is to guide the fluid and manage flow distribution, and numerous studies corroborate their potential benefits. For instance, splitter blades have been shown to improve flow distribution within centrifugal pump impellers. Research by [33], cited in, utilized CFD to analyze internal flow characteristics as influenced by impeller design, including splitters. Similarly, [34] demonstrated that splitter blades in Francis turbines could effectively reduce pressure fluctuations in the vaneless space and alter the blade passing frequency, indicative of flow modification. Further supporting this, studies by [35] found that the addition of short blades or splitter blades can improve the impeller's internal flow field distribution and suppress flow separation, leading to enhanced velocity distribution uniformity by as much as 17%. The basic premise that a single splitter divides the flow into two distinct paths aligns with the primary mechanical function of such a component.

4.2. Effect of Cone Size on Volume Flow Rate and Efficiency

The study investigated the influence of separate factors on volume flow rate and used the Response Surface Methodology (RSM). This work explores torque (A), bypass angle (B), and turbine cone size (C) as independent factors. The volume flow rate (Y) is now selected to serve as the dependent variable (response). CCD is set in four categorical parameters with eight test points and three experimental replicas for every category that comprise the intended model; this study consists of 44 total experimental tests, as suggested by RSM. Table 1 represents the test run models of experimental design factors and experimental responses.

Table 1. CCD experimental design variables and practical responses

Run	Torque (N-m)	Bypass Angle (°)	Turbine Type (In.)	Volume Flow Rate (m^3/hr)	Efficiency (%)	Run	Torque (N-m)	Bypass Angle (°)	Turbine Type (In.)	Volume Flow Rate (m^3/hr)	Efficiency (%)
1	60	45	3.25 cone	53.31	71.341	23	40	45	3.25 cone	53.31	51.1173
2	20	67.5	3.25 cone	50.2	32.5322	24	60	45	2.25 cone	55.34	78.3047
3	20	45	3.25 cone	53.31	32.48439	25	40	45	2.25 cone	55.34	49.7727
4	40	45	2.75 cone	65.17	47.949	26	20	67.5	2.75 cone	55.3	32.18299
5	40	67.5	2.25 cone	52.55	49.356	27	20	22.5	2.75 cone	75.69	32.43036
6	40	67.5	0 cone	55.16	67.9742	28	60	67.5	2.25 cone	53.5	64.6258
7	60	67.5	0 cone	54.18	68.6611	29	60	67.5	3.25 cone	49.51	61.1847
8	20	22.5	2.25 cone	79.74	31.72841	30	40	45	2.25 cone	56.3	49.4356

9	40	45	3.25 cone	53.31	51.1173	31	40	67.5	3.25 cone	49.51	52.3544
10	40	45	2.75 cone	65.17	47.949	32	20	22.5	0 cone	71.63	32.2608
11	60	22.5	0 cone	70.63	79.5106	33	60	22.5	2.25 cone	79.74	75.1307
12	20	67.5	0 cone	54.18	32.21771	34	60	67.5	2.75 cone	55.3	58.7752
13	40	22.5	2.25 cone	80.1	43.7149	35	40	45	2.75 cone	65.17	47.949
14	40	45	0 cone	60.18	47.5821	36	20	67.5	2.25 cone	53.55	32.21988
15	20	22.5	3.25 cone	67.21	32.6372	37	20	45	2.75 cone	65.17	32.1175
16	60	22.5	2.75 cone	75.69	77.1886	38	40	45	0 cone	60.18	47.5821
17	40	45	2.25 cone	55.34	49.7727	39	40	22.5	2.75 cone	75.69	45.0223
18	40	67.5	2.75 cone	55.3	48.4536	40	20	45	2.25 cone	56.34	32.39625
19	60	45	2.75 cone	65.17	67.1669	41	60	45	0 cone	60.2	78.5027
20	20	45	0 cone	60.2	31.92019	42	40	45	0 cone	61.1	47.3173
21	40	22.5	3.25 cone	67.21	46.9366	43	40	22.5	0 cone	70.63	46.4099
22	40	45	3.25 cone	53.31	51.1173	44	60	22.5	3.25 cone	67.21	51.1173

The experimental results were studied to create a regression model. Responses along with the results of ANOVA were analyzed at this time. A sketch of that response surface model was analyzed at this time, too. In this analysis, "Design Expert 12" software was used. As suggested, the software translated Equations 6, 7, 8, and 9, presenting the most important models based on different CESRT turbine cone sizes.

$$0-\text{in Cone: Volume Flow Rate } (Y) = 58.64 - 1.142 \times 10^{-1} \times A - 10.12 \times B + 1.62 \times 10^{-2} \times AB + 1.89 \times 10^{-2} \times A^2 + 4.66 \times B^2 \text{ n} \quad (6)$$

$$2.25-\text{in Cone: Volume Flow Rate } (Y) = 1.84 - 5.25 \times 10^{-2} \times A + 1.89 \times B + 2.337 \times 10^{-1} \times AB - 2.811 \times 10^{-1} \times A^2 - 2.22 \times B^2 \quad (7)$$

$$2.75-\text{in Cone: Volume Flow Rate } (Y) = -3.01 - 6.08 \times 10^{-2} \times A - 3.21 \times B - 2.87 \times 10^{-2} \times AB - 2.282 \times 10^{-2} \times A^2 + 6.07 \times B^2 \quad (8)$$

$$3.25-\text{in Cone: Volume Flow Rate } (Y) = 6.53 + 1.142 \times 10^{-1} \times A - 7.29 \times B - 1.62 \times 10^{-2} \times AB - 1.89 \times 10^{-2} \times A^2 - 4.33 \times B^2 \quad (9)$$

A and B are coded values relating to torque and bypass angle, A2 and B2 are squared terms relating to the studied parameters, and AB is an interaction term. These equations model the volume flow rate (Y) for turbines, with varying cone diameters, disclosing a complex relationship between the variables A and B and the resulting flow. Equation 6 shows a high basal flow rate for the 0-inch cone, which decreases as either A or B do. However, the two variables interact, and the quadratic terms may positively affect the flow rate. The baseline flow decreases substantially when Equation 7 is applied to a 2.25-inch cone. B now positively influences the flow, and both A and B exhibit an optimal range as a result of negative quadratic terms. The baseline flow in Equation 8 is negative, and both A and B have a negative impact on flow.

However, the quadratic elements indicate potential increases at higher values. This is the case when a 2.75-inch cone is used. Lastly, Equation 9, which is applicable to a 3.25-inch cone, reverts to a positive baseline. The flow is positively influenced by A and negatively influenced by B, and both variables are once again within an optimal range as a result of the negative quadratic terms. Collectively, these equations illustrate the substantial impact of cone size on turbine performance and the intricate relationship between variables A and B in determining volume flow rate.

Table 2. ANOVA table for the volume flow rate

Source	Sum of Squares	df	Mean Square	F-value	p-value	
Model	3437.75	23	149.47	992.19	< 0.0001	significant
A-Torque	0.3128	1	0.3128	2.08	0.1651	
B-By-pass Angle	2458.96	1	2458.96	16323.03	< 0.0001	
C-Turbine Size	476.55	3	158.85	1054.47	< 0.0001	
AB	0.0042	1	0.0042	0.0280	0.8687	
AC	0.1170	3	0.0390	0.2588	0.8542	
BC	94.84	3	31.61	209.85	< 0.0001	
A^2	0.0036	1	0.0036	0.0241	0.8781	
B^2	219.83	1	219.83	1459.30	< 0.0001	
ABC	0.3654	3	0.1218	0.8086	0.5039	
A^2C	0.3460	3	0.1153	0.7655	0.5267	
B^2C	154.16	3	51.39	341.12	< 0.0001	

Residual	3.01	20	0.1506			
Lack of Fit	1.83	12	0.1529	1.04	0.4953	not significant
Pure Error	1.18	8	0.1473			
Cor Total	3440.77	43				

The ANOVA in Table 2 reveals a highly significant model ($p < 0.0001$, $F = 992.19$) for predicting volume flow rate, indicating that the included factors substantially influence the outcome. Among the individual factors, Bypass Angle (B) and Turbine Size (C) exhibit highly significant effects ($p < 0.0001$), with Bypass Angle demonstrating a powerful influence ($F = 16323.03$). Torque (A) shows no significant individual effect ($p = 0.1651$). Several interaction terms demonstrate significance, including BC and B^2C, highlighting the complex interplay between these factors.

Additionally, the quadratic term B^2 is significant, indicating a non-linear relationship with the flow rate. Notably, the BC and B^2C interactions are significant, further emphasizing the intricate nature of the relationships. Conversely, AB, AC, ABC, A^2C, and A^2 interactions are not significant. The residual variance is relatively low (0.1506), suggesting a good fit of the model to the data. The bypass angle and turbine size are primary drivers of volume flow rate, with significant interaction and quadratic effects contributing to the overall model complexity. The lack of fit is not significant ($p = 0.4953$). The R^2 value (coefficient of determination) showed variance in the model's designed data. R^2 predicts the proportion of the variance within the dependent variable (response) from the independent variable (predictors). The model fits the data suitably in the event that R^2 approaches one. This proximity does suggest that the model has a strong fit. As assessed by the ANOVA in Table 3, the response surface designed model demonstrates exceptional statistical performance. The model exhibits a very high coefficient of determination (R^2) of 0.9991, indicating that 99.91% of the variability in the response is explained by the model, signifying an excellent fit. The adjusted R^2 of 0.9981, closely aligned with the R^2 value, confirms that the model is not overfitted and includes relevant predictors.

Furthermore, the predicted R^2 of 0.9937 underscores the model's robust predictive capability for new observations. The model's reliability is further supported by an Adeq Precision value of 106.8269, indicating a very strong signal-to-noise ratio, making it exceptionally suitable for navigating the design space. A low standard deviation of 0.3881 and a coefficient of variation (C.V.) of 0.6343% suggest very high precision and low variability relative to the mean response of 61.19. These metrics confirm that the response surface model is highly accurate, reliable, and exceptionally well-suited for prediction and optimization purposes.

Table 3. Response surface designed model of CESRT

Factors	%
R^2	0.9991
Adjusted R^2	0.9981
Predicted R^2	0.9937
Adeq Precision	106.8269
Std. Dev.	0.3881
Mean	61.19
C.V.	0.6343

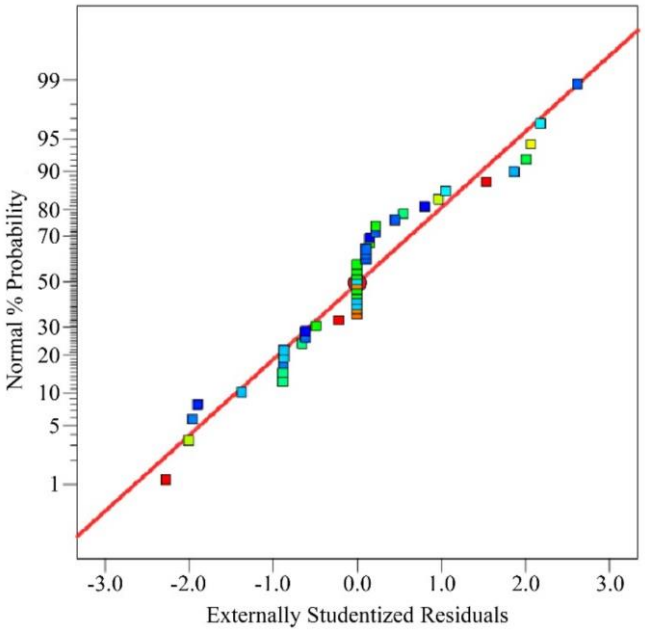

(a)

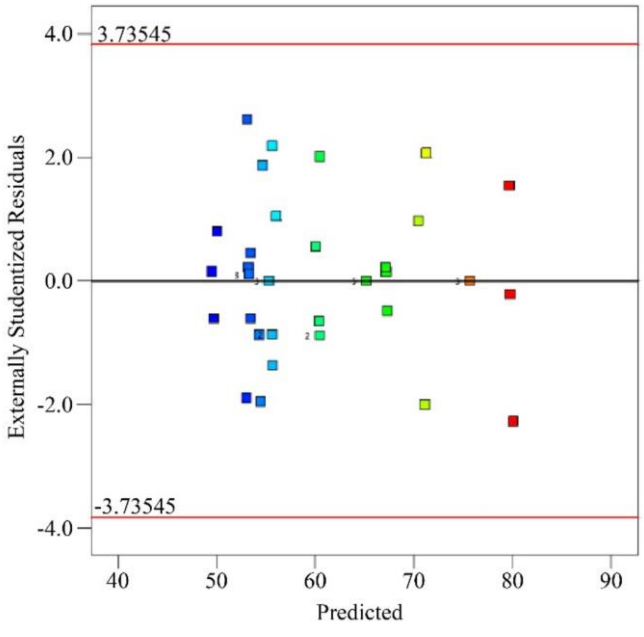

(b)

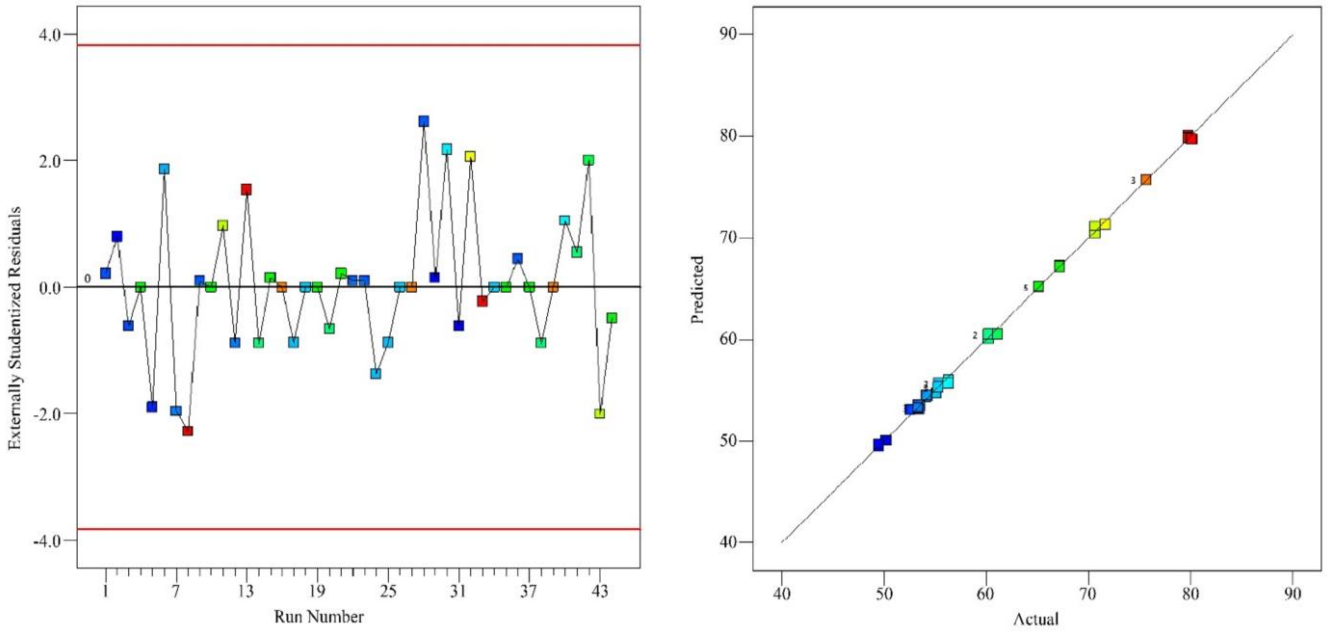

(c) (d)

Fig. 4 The regression model's validity of CESRT, (a) Externally studentized residuals vs. Normal probability, (b) Predicted vs. Externally studentized residuals, (c) Number of runs vs. Externally studentized residuals and, (d) Actual vs. Predicted.

The regression model's validity was evaluated through a series of diagnostic plots shown in Figure 4(a), (b), (c), (d). Figure 4(a) shows the standard probability plot vs. externally studentized residuals, demonstrating that the residuals were approximately normally distributed, fulfilling a key assumption of linear regression.

Figure 4(b), the residuals vs. predicted values plot, exhibited a random scatter of residuals around zero, indicating homoscedasticity and suggesting the absence of non-linearity. Similarly, Figure 4(c) shows the residuals vs. run order plot, revealing random fluctuation, supporting the assumption of independence of errors, and indicating no discernible time-related or carryover effects. Finally, Figure 4(d) shows the predicted vs. actual plot, illustrating a strong correlation between predicted and observed values, with points clustered tightly around the diagonal line, signifying a good model fit and accurate prediction. These plots provided visual confirmation that the regression model met the necessary assumptions and effectively captured the relationship between the variables under study. Thus, according to the ANOVA analysis results, the CESRT experimental data were fitted to the designed model. The volume flow rate for CESRT can be predicted by a valid model that is offered.

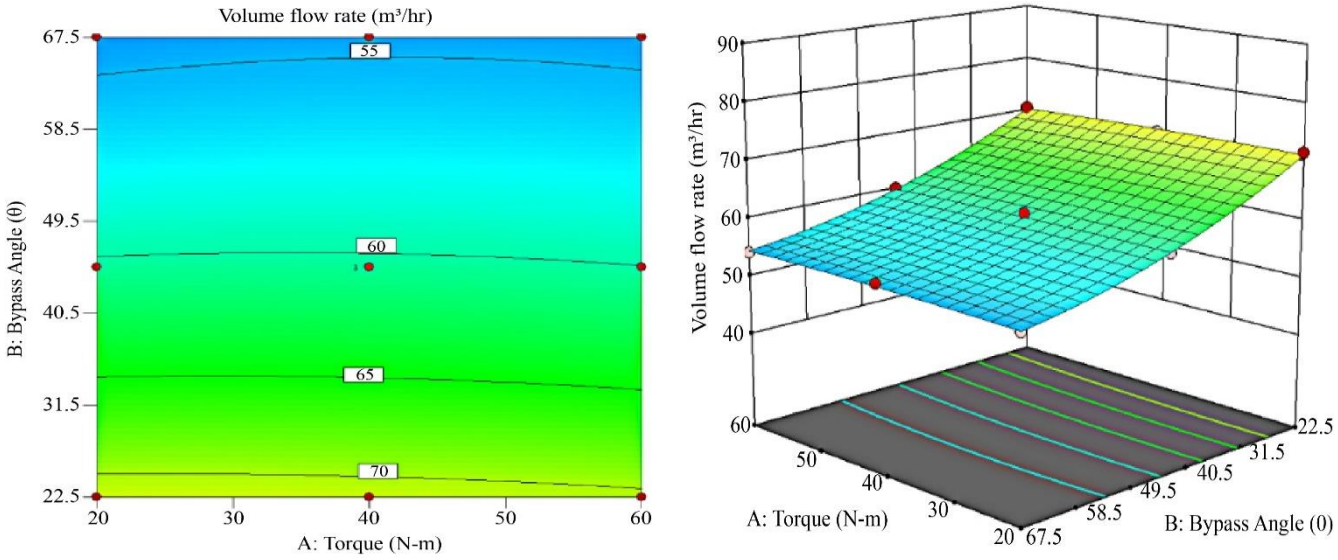

(a)

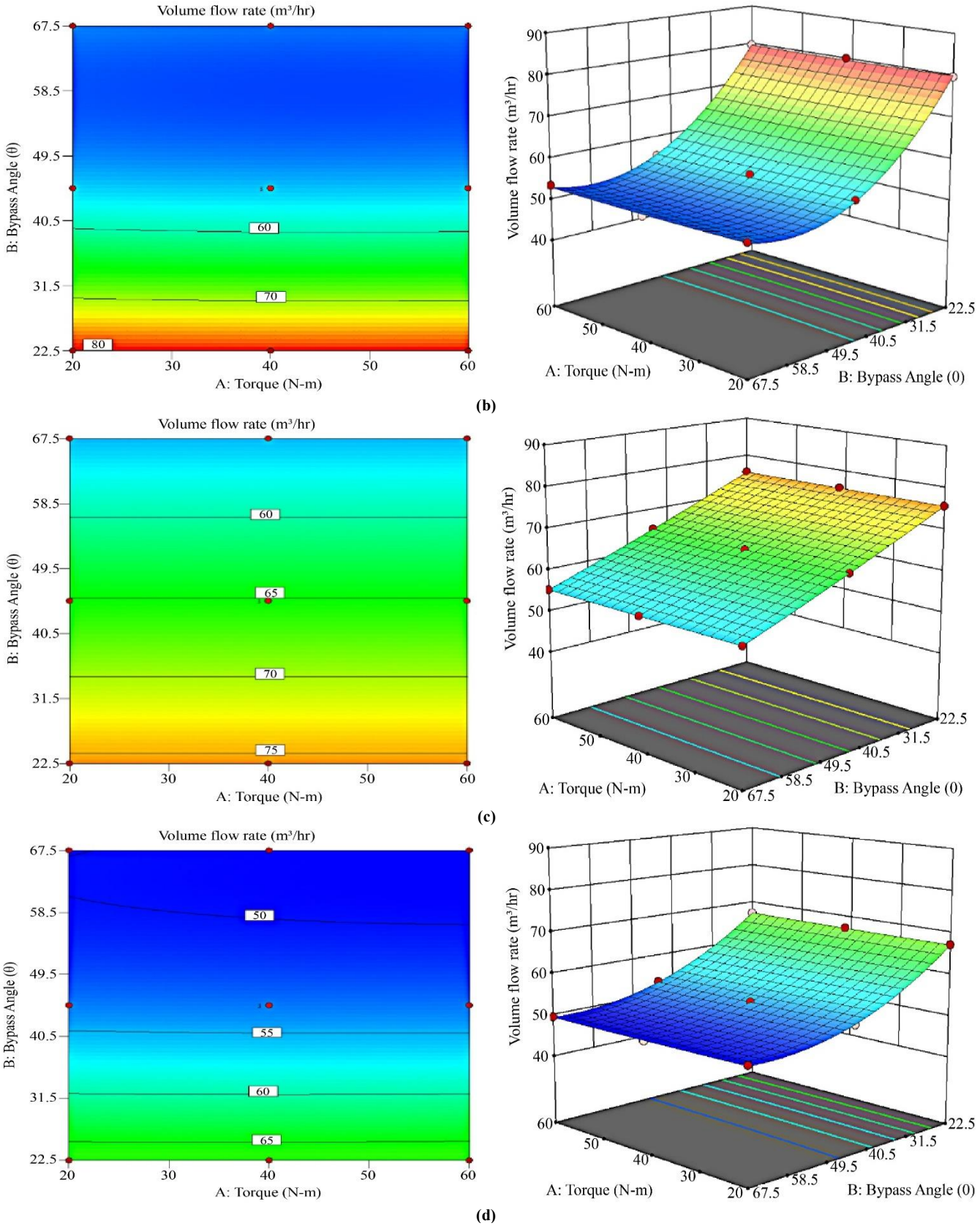

Fig. 5 The response surface and contour plots of volume flow rate as a function of torque (N-m) and bypass angle (θ) in different turbine cone sizes of (a) 0-in cone, (b) 2.25-in cone, (c) 2.75-in cone, and, (d) 3.25-in cone.

The investigation of the impact of cone size on the relationship between torque, bypass angle, and volume flow rate, utilizing contour and 3D surface plots for visualization, is shown in Figure 5 (a), (b), (c), (d). Four different cone sizes were examined: 0 inches, 2.25 inches, 2.75 inches, and 3.25 inches. Across all cone sizes, a consistent trend emerged: increasing both torque and bypass angle generally resulted in a higher volume flow rate.

However, the magnitude of this effect varied significantly depending on the cone size. The 0-inch cone, represented in Figure 5(a), exhibited the lowest torque and bypass angle changes sensitivity. This trend is visually apparent in the relatively shallow slopes of the 3D surface plot and the gradual color transitions in the contour plot.

In contrast, Figure 5(b), the 2.25-inch cone, demonstrated a marked increase in sensitivity, with a steeper 3D surface plot and a more pronounced color gradient in the contour plot, indicating a more significant response to torque and bypass angle adjustments. Interestingly, the 2.75-inch cones in Figure 5(c) and 3.25 inches in Figure 5(d) exhibited a similar sensitivity to the 2.25-inch cone, suggesting a potential plateau in the response.

This plateau implies that cone size gains beyond 2.25 inches may not gain the needed ability to control volume flow rate through the manipulation of torque and bypass angle. This phenomenon might be attributed to factors such as the system's fluid dynamics or the cone's specific geometry, and it warrants further investigation. The choice of the 2.25-inch cone is the most effective kind. We must consider the sensitivity together with the potential plateau balance.

It greatly increases sensitivity versus the 0-inch cone, so it allows more precise control over the volume flow rate. At the same time, it avoids the diminishing returns observed with larger cone sizes, where further increases in sensitivity are minimal. The RSM analysis, the deviation curves for volume flow rate responses with coded factors are shown in Figure 6 (a), (b), (c), (d).

Figure 6 revealed a critical influence of cone size on the relationship between bypass angle and volume flow rate. Specifically, Figure 6(a) shows the 0-inch cone and Figure 6(c) shows the 2.75-inch cone; the bypass angle exhibited a clear linear inverse relationship with the flow rate.

This implies that increasing the bypass angle within these configurations leads to a proportional decrease in the volume flow. Conversely, Figure 6(b) represented the 2.25-inch cone, and Figure 6(d) showed the 3.25-inch cone; a non-linear pattern emerged. An initial increase in bypass angle resulted in a sharp reduction in flow, followed by a plateau and a slight subsequent increase. This suggests a more complex interaction between the bypass angle and the flow dynamics at these larger cone sizes. Torque, representing a potentially independent operational parameter, consistently showed minimal impact on the volume flow rate across all cone configurations, as indicated by the near-horizontal lines in all figures.

Furthermore, the torque and bypass angle interaction was negligible for the 0-inch and 2.75-inch cones. In contrast, a potential, though likely weak, interaction was observed for the 2.25-inch and 3.25-inch cones, as evidenced by the slightly non-parallel lines.

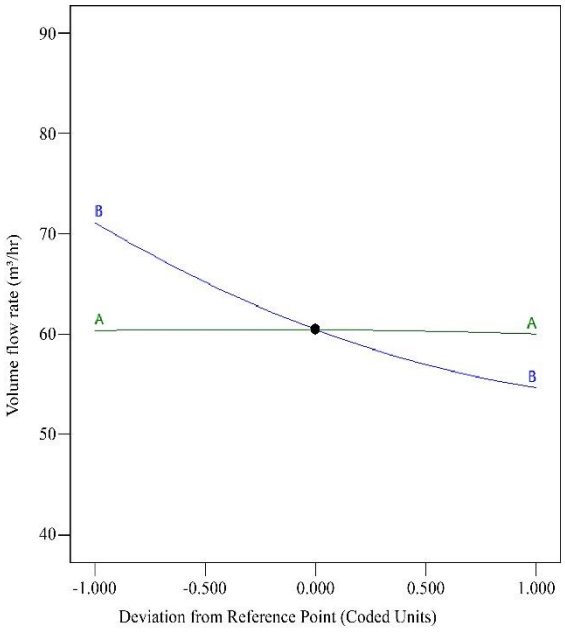

(a)

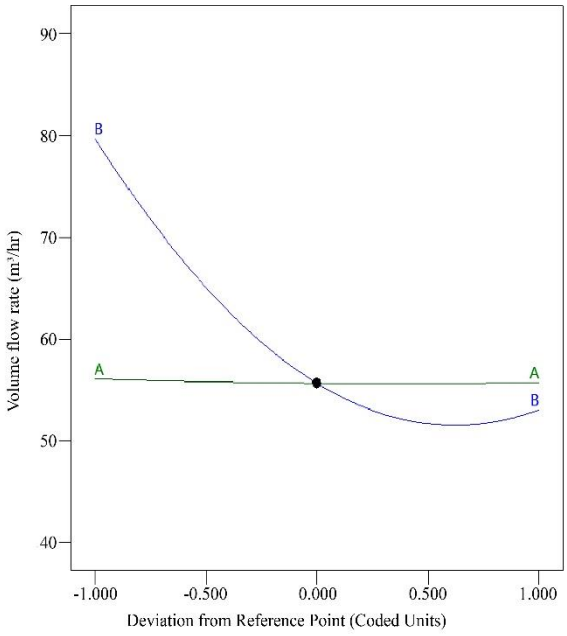

(b)

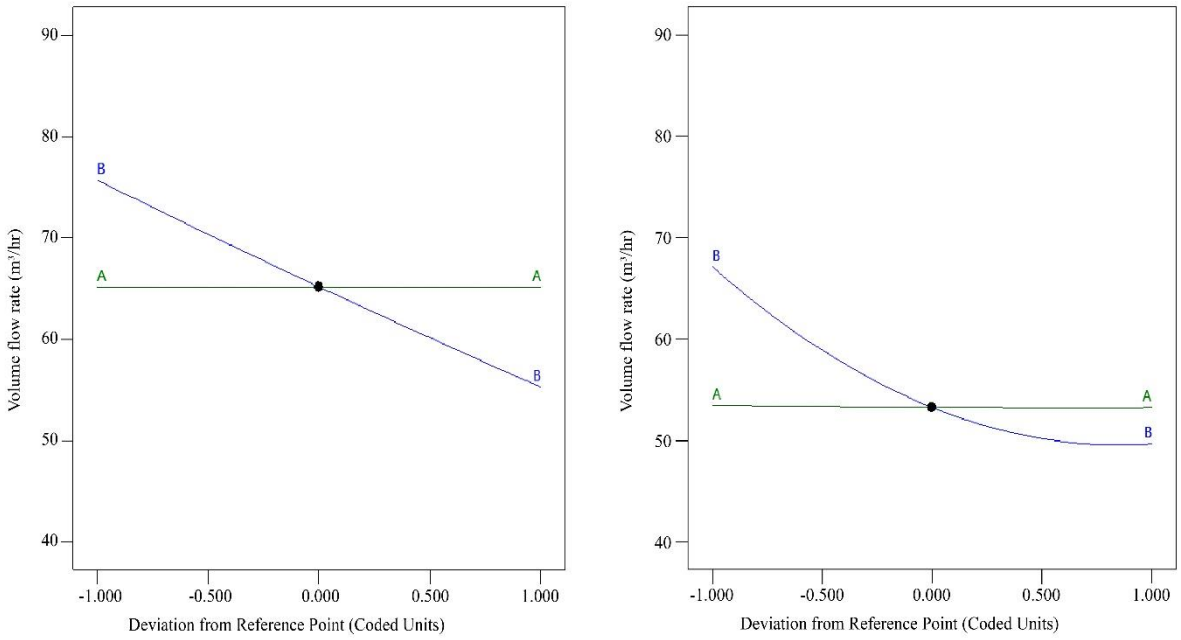

Fig. 6 Deviation curves for volume flow rate responses with coded factors for (a) 0-in cone, (b) 2.25-in cone, (c) 2.75-in cone, and (d) 3.25-in cone, types of turbines

Table 4. Optimal values of the designed metrics and response of CESRT

Metrics	Target	Minimum	Maximum	Optimal Values
Torque (N-m)	In range	20	60	60
Bypass Angle (º)	In range	22.5º	67.5º	22.5º
Turbine Cone size (in)	In range	0-in cone, 2.25-in cone, 2.75-in cone, 3.25-in cone		2.25-in cone
Volume flow rate (m^3/hr)	Maximum	49.51	80.1	79.7799
Efficiency (%)	Maximum	31.72841%	80.0319%	77.0772%
Desirability	-	0	1	0.964

Table 5. Comparison of volume flow rate between experimental and RSM results

	Volume flow rate (N-m)		
	Result of Experiment	**Result of RSM**	**Percentage Error (%)**
1 Torque = 60 By-pass Angle = 22.50° Cone Size = 2.25	79.10	79.7799	0.8522%

4.3. Optimum Conditions for Efficiency and Flow Rate

Investigating the best volume flow rate intends to find the design parameters. The volume flow rate operates optimally upon setting these parameters. Table 4 shows all of the designed parameters as well as the required model response details for the CESRT's optimization process. For the optimization, the two responses that are shown in Table 4 are efficiency and volume flow rate.

The reactions were set for maximum value, while the input parameters were in a specified range. These conditions show that the optimum torque exists at 60 N-m, as a bypass angle exists at 22.5°, and a turbine cone size exists at 2.25-in cone. The maximum volume flow rate reached is 79.779 m³/hr, and the turbine efficiency is 77.0772%. Figure 7 illustrates the output results of the designed model, which are nearly identical to the utmost expectation established for the model. The desirability value is represented as a variable ranging from 0 to 1, indicating the degree to which the output is similar to the desired output.

The desirability value of 0.964 is a favorable outcome for optimization, as it indicates that the designed factors are optimally configured to ensure the responses. The experimental results are contrasted with the RSM model results, as illustrated in Table 5, to verify the optimal conditions for the designed parameters.

The confirmation test indicates that the reported error (0.8522%) between the actual and predicted power ratio is negligible, indicating a satisfactory match between the experimental tests and the designed RSM model.

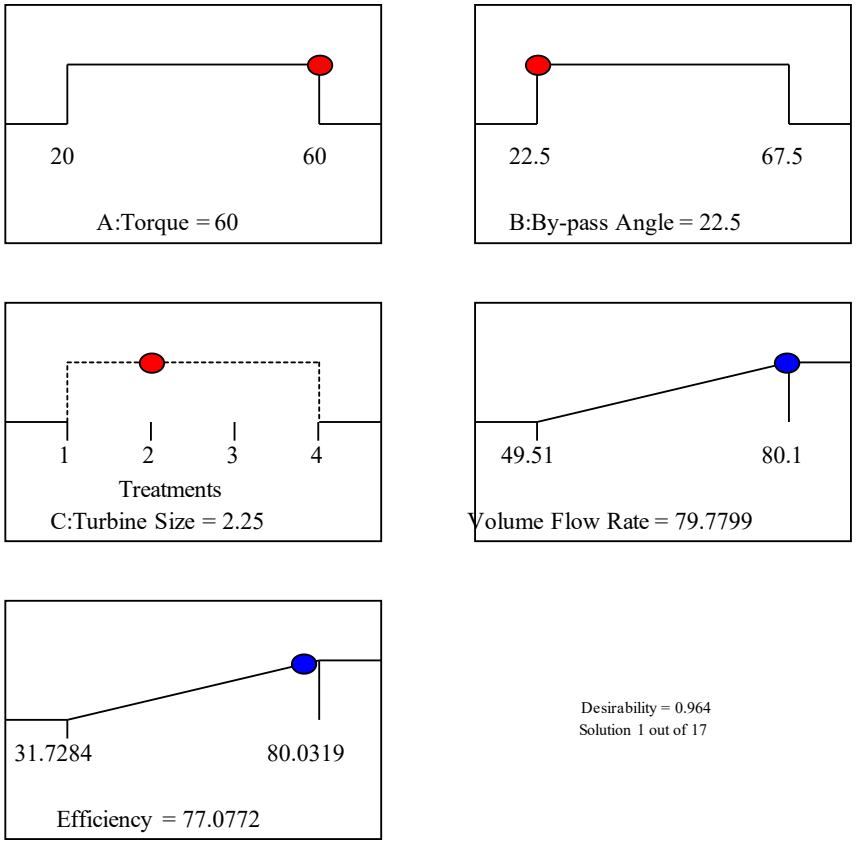

Fig. 7 Desirability for optimization of parameters for maximum volume flow rate and efficiency

4.4. Analysis of Cone Size on Efficiency vs. Flow Rate Performance

Figure 8 presents the plot of efficiency versus flow rate of CESRT. The performance curve attributed to the 3.25-in cone generally repre sents the lower boundary of efficiency across the tested flow rates. While it follows the general trend of increasing efficiency with increasing flow, its rise is less pronounced compared to the other configurations. It struggles to surpass approximately 71% efficiency, even at higher flow rates. This suggests that the 3.25-inch cone, being the largest, likely introduces significant hydraulic losses within the turbine housing. These losses may stem from increased flow obstruction, which could lead to higher internal turbulence and friction, or it might alter the flow path to prevent the water jet from impacting the turbine's reaction surfaces at an optimal angle or velocity. This configuration appears to be sub-optimal for effective energy conversion in this specific turbine design across all tested flow conditions. The 2.75-in cone demonstrates a noticeable improvement over its 3.25-in counterpart. Its efficiency curve rises more steeply and reaches higher peak values, likely achieving around 77% efficiency at the upper end of the flow rate range. This indicates that reducing the cone size from 3.25 to 2.75 inches successfully mitigates some of the hydraulic losses observed with the larger cone. It appears to strike a better balance, potentially guiding the flow more effectively towards the reaction surfaces without imposing as much detrimental obstruction. This configuration represents a viable, though not the best, operational choice, particularly at higher flow rates. The baseline configuration, the 0-in cone, performs remarkably well, achieving one of the highest peak efficiencies, likely reaching close to 80% at flow rates exceeding 70 m^3/hr. Its curve shows a strong and relatively steady increase in efficiency as the flow rate rises. This high performance can be attributed to the minimal internal obstruction in this setup. Without a cone, the water flow experiences less friction and potentially less turbulence generated by an internal structure, allowing for a very direct (though perhaps less guided) conversion of kinetic energy. This highlights the inherent effectiveness of the basic Split Reaction Turbine design and sets a high benchmark for surpassing any proposed enhancements, like the cone. The curve inferred to represent the 2.25-in cone confirms its status as the optimal design identified through the RSM analysis.

It consistently tracks near the top of the performance range, closely matching or even slightly exceeding the 0-in cone's efficiency at various points, and achieving peak efficiencies likely around 78%. Importantly, it appears to maintain high efficiency over a broader range of high flow rates compared to other configurations. This suggests that the 2.25-in cone strikes the most effective balance: it is large enough to guide and concentrate the flow onto the reaction surfaces successfully-likely improving the quality of the

energy transfer-yet small enough to avoid introducing significant parasitic losses through obstruction and turbulence. This ability to enhance flow dynamics without undue penalty makes it the most promising configuration for maximizing the overall performance and operational flexibility of the CESRT in pico-hydro applications.

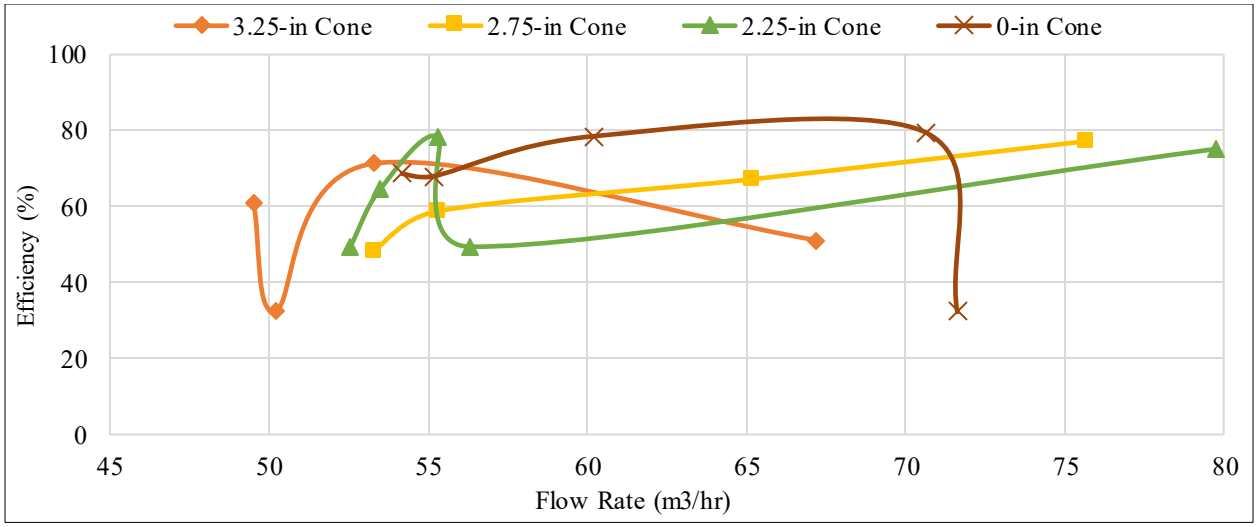

Fig. 8 Efficiency versus flowrate of CESRT

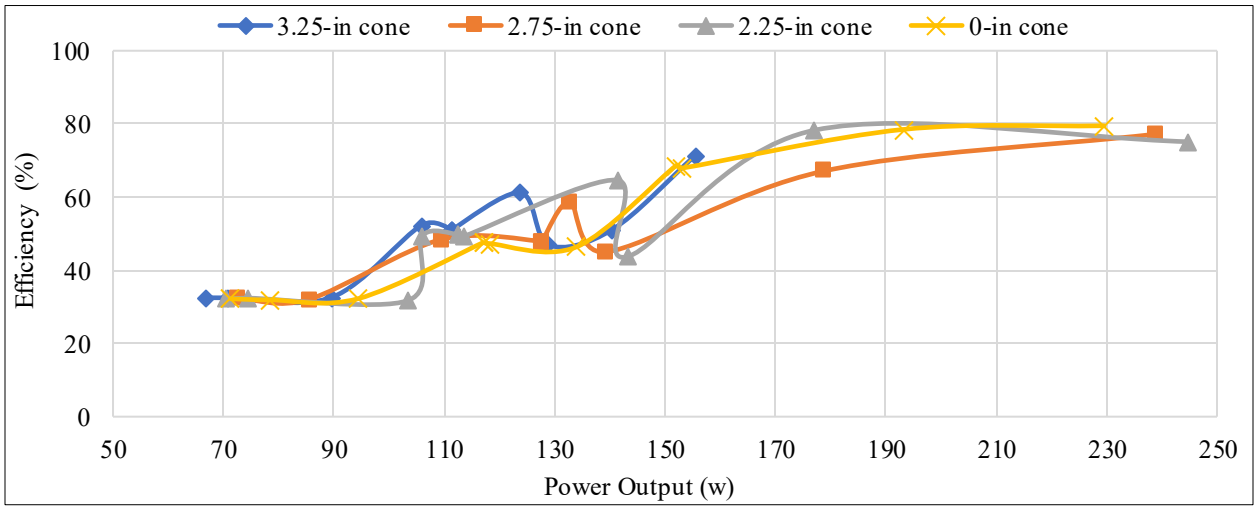

Fig. 9 Plot of power output vs. Efficiency of CESRT

4.5. Individual Cone Performance: Efficiency vs. Power Output

Figure 9 depicts the cone performance of CESRT in terms of efficiency versus power output. The 3.25-in cone configuration, as inferred from its performance curve, generally represents the lower boundary in terms of both maximum power output and achievable efficiency. Its curve (likely the lowest and shortest in Figure 3) shows a modest increase in efficiency as power increases. However, it peaks at a relatively low power output (around 155 W) and achieves a maximum efficiency of only about 71.3%. This suggests that while it can operate, its large size likely creates significant hydraulic drag and obstruction, preventing the turbine from reaching the higher power and efficiency levels seen with other designs. Its operational range appears limited, making it the least favorable option among those tested. The 2.75-in cone shows a significant improvement over the 3.25-in version. Its corresponding curve likely demonstrates a much wider power range, extending towards 239 W, while achieving a respectable peak efficiency of approximately 77.2%. The curve shows a strong positive correlation, indicating that this cone performs best at higher power outputs. This suggests that the 2.75-in cone offers a better compromise between flow guidance and obstruction than the 3.25-in cone, allowing the turbine to convert more hydraulic energy into power, especially under high load conditions. The baseline 0-in cone configuration exhibits a compelling performance curve. It achieves the highest peak efficiency observed, reaching approximately 79.5% at a substantial power output of around 230 W. Furthermore, it maintains high efficiency (over 67%)

even at intermediate power levels (around 150 W). This curve indicates that the basic Split Reaction Turbine design is inherently capable, particularly in terms of efficiency.

The lack of an internal cone means minimal internal obstruction, allowing for high efficiency, though perhaps with less flow control compared to an optimized cone, which might explain why it does not reach the absolute highest power output. The performance curve attributed to the 2.25-in cone strongly supports its selection as the optimal configuration in the RSM analysis. It achieves the highest power output, reaching nearly 245 W. While its peak efficiency (around 78.3%) is marginally lower than the 0-in cone's peak, it achieves this high efficiency at a substantial power level (around 177 W) and maintains strong efficiency (over 75%) even at its maximum power output. This curve represents the best overall balance - delivering very high power and efficiency. It demonstrates that the 2.25-in cone optimises the internal flow dynamics, concentrating the flow on the turbine's reaction surfaces to maximize power extraction without introducing prohibitive hydraulic losses, thereby maximizing efficiency across a wide, high-performance range.

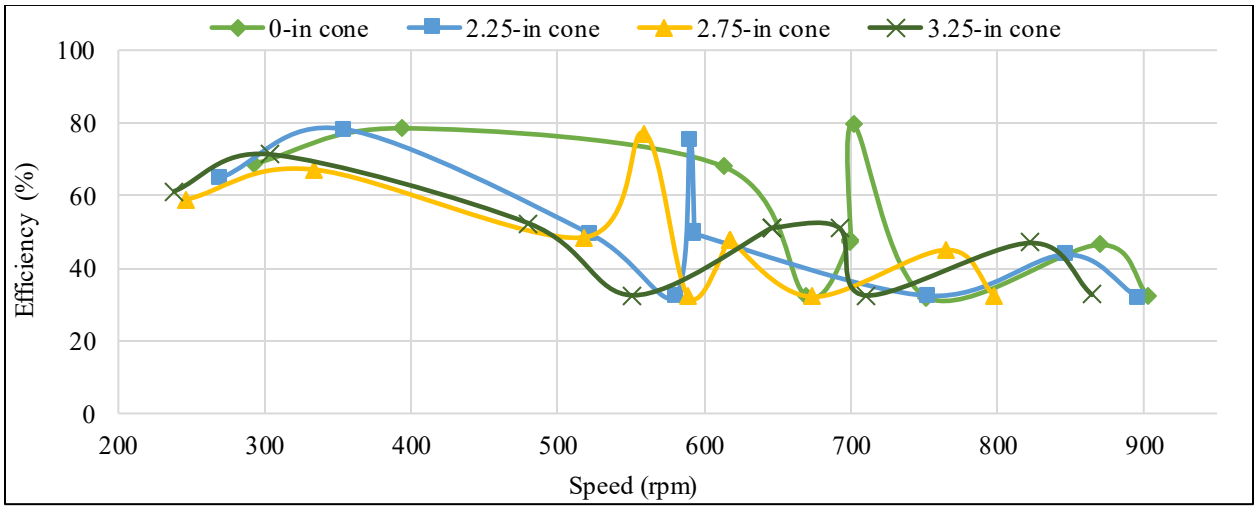

Fig. 10 Plot of efficiency versus speed of CESRT

4.6. Exploring the Efficiency-Speed Relationship for Each Cone Size

A common characteristic observed in Figure 10 for all configurations is the presence of a distinct peak efficiency at a specific rotational speed. This is typical for turbomachinery, where performance is maximized when the fluid velocity, blade angle, and rotational speed align optimally. At speeds below the optimum, the turbine may not be effectively capturing the fluid's momentum. In contrast, at speeds above the optimum, hydraulic losses due to factors like increased friction, turbulence, or inefficient fluid-blade interaction tend to increase, causing efficiency to drop. The curve inferred to represent the 3.25-in cone consistently shows the lowest efficiency across the range of speeds. Its peak efficiency appears lower than the others and potentially occurs at a lower rotational speed. This behavior reinforces the idea that the largest cone creates significant internal drag and flow obstruction. As the turbine attempts to spin faster, these resistive forces likely increase substantially, rapidly diminishing the efficiency and limiting the achievable speed, thus providing the least effective performance in terms of speed and efficiency. The 2.75-in cone likely corresponds to one of the intermediate curves, demonstrating improved performance compared to the 3.25-in cone. It likely achieves a higher peak efficiency and maintains it over a slightly broader speed range. This suggests that the reduced size lessens the negative impacts of drag at higher speeds, allowing the turbine to operate more efficiently as it spins faster, up to its optimal point. It represents a workable, but not superior, design in terms of its speed efficiency profile. The 0-in cone (baseline) configuration likely represents one of the top-performing curves. Given its high peak efficiency seen in previous analyses, it probably reaches a high efficiency level, perhaps over a relatively wide speed range or peaking at a significant speed. The absence of a cone means lower rotational drag, potentially allowing it to achieve higher speeds more easily while maintaining good efficiency.

This makes it an attractive option, especially if high rotational speeds are desired for direct generator coupling. The 2.25-in cone, identified as optimal via RSM, is expected to exhibit a strong performance curve, likely achieving a high peak efficiency comparable to or just below the 0-in cone. Crucially, its peak might occur at a very practical and effective speed and may maintain high efficiency over a reasonably wide operational speed band. This indicates that the 2.25-in cone provides effective flow management - guiding the water to produce torque efficiently - without introducing excessive drag that would penalize performance at higher speeds. A broad, high peak is often desirable in real-world applications where operating conditions (and thus optimal speed) can fluctuate. This robust speed efficiency characteristic further

validates the 2.25-in cone as the most suitable design for the CESRT.

4.7. Comparative Results of the Present Study

The enhanced efficiency of 77.0772% achieved in the present study with the Cone-Enhanced Split Reaction Turbine (CESRT), as highlighted in Table 6, marks a notable advancement when compared to the 65% to 70% efficiencies reported in the foundational works on Split Reaction Turbines (SRTs) by [5-7]. This improvement is primarily rooted in a more specialized and in-depth optimization approach focusing on both novel internal geometric modifications and specific operational parameters, a level of detail not explored in the earlier SRT research. The present study's introduction of a cone size as a distinct design element within the turbine, coupled with the systematic investigation of its interaction with torque and bypass angle through Response Surface Methodology (RSM), is a key differentiator. In contrast, the previous studies by [5-7], while crucial for establishing the viability of the SRT concept with efficiencies around 65-70%, primarily investigated broader parameters such as head, flow rate and nozzle diameter for the standard SRT design. These earlier works laid the groundwork by demonstrating the SRT's potential for low-head micro-hydro installations and its simpler manufacturing process, often involving splitting PVC pipes and offsetting the halves to create nozzles.

The SRT itself represented an evolution in simple reaction turbines, aiming to overcome limitations of earlier designs like the Cross Pipe Turbine (CPT). The CPT, often constructed from standard galvanized steel pipe fittings, faced challenges in achieving smaller rotor sizes and flexible nozzle exit areas due to the fixed dimensions of its components [8]. The SRT addressed some of these issues by allowing for more adaptable construction. However, as investigated by [5-7], the standard SRT still had areas for potential refinement, which the present study on the CESRT has addressed. The cone-shaped insert in the CESRT is a specific internal modification specifically intended to optimize turbine performance by strategically directing and concentrating water flow towards the turbine cones, thereby significantly altering the internal flow dynamics. This targeted geometric enhancement, particularly the finding that the 2.25-inch cone provides the most efficient performance, combined with the rigorous multi-parameter optimization using RSM to identify optimal settings for torque (60 N-m) and bypass angle (22.5°), allowed the CESRT to achieve a higher efficiency.

This contrasts with other simple reaction turbines discussed in literature, such as Quek's turbine [2], which, despite being a reaction type, involved complex manufacturing and showed lower efficiencies (less than 45%) even at higher heads, or Whitlaw's Mill, which featured curved arms but did not gain significant traction. Even the Z-Blade turbine, a more recent development aiming for utmost simplicity and high efficiency by using standard PVC fittings and easily modifiable nozzles, highlights the ongoing pursuit of performance improvements in simple reaction turbines [2]. The present study's success with the CESRT, therefore, stems from its focused approach on a novel internal component (the cone) and the detailed statistical optimization of its interplay with operational parameters. This approach moves beyond the general design and broader parametric evaluations of the SRTs in previous works and other earlier reaction turbine designs.

Table 6. Comparative overview of simple reaction turbines for pico-hydropower

No. of References	Type of Turbine	Efficiency
[2]	Quek's turbine	<45%
[8]	Cross Pipe Turbine (CPT)	~53%
[2]	Z-Blade Turbine	Up to 78-82%
[5-7]	Split Reaction Turbine (SRT)	65-70%
Present Study	Cone-Enhanced Split Reaction Turbine (CESRT)	77.0772%

5. Conclusion

This study successfully showed that the performance of a Split Reaction Turbine (SRT) is improved when a cone-shaped insert is incorporated, creating the Cone-Enhanced Split Reaction Turbine (CESRT). It successfully investigated the relationship between water flow rate and the efficiency of a cone-enhanced simple-split reaction water turbine using a Response Surface Methodology (RSM). The model was statistically significant with an R^2 value of 0.9991, as indicated by the ANOVA analysis, and could be used to predict the volume flow rate of the turbine. The results showed that the cone size significantly impacted the volume flow rate, with the 2.25-inch cone providing the most efficient performance. The bypass angle also considerably affected the flow dynamics, particularly for larger cone sizes. The study also found that torque had minimal impact on the volume flow rate across all cone configurations.

The optimum volume flow rate and efficiency conditions were achieved at a torque of 60 N-m, a bypass angle of 22.5°, and a 2.25-in cone turbine type. The maximum achieved volume flow rate and the turbine's efficiency were 79.7799

m^3/hr and 77.0772%, respectively. The study showed that the model was accurate with a small error of 0.8522%, and these settings reached a maximum efficiency of 77.0772%, which is better than the usual 65-70% seen in standard SRTs.

The RSM model was validated through experimental tests, demonstrating a satisfactory correlation between predicted and actual results. This research ultimately validates the CESRT as a superior design offering strong, data-driven guidelines that are important for sustainable energy in remote communities and for developing more effective pico-hydropower systems.

Acknowledgments

The researchers would like to express our sincere gratitude to our adviser, Dr. Sherwin A. Guirnaldo, for imparting his knowledge and wisdom about this project and also for his guidance, encouragement, understanding and patience in completing this work; To our esteemed and extraordinary panellists: Engr. Abdulrahman C. Manalundong, Engr. Abdullah D. Lomondaya, and Engr. Joseph Lester F. Galindo's expertise and guidance have contributed significantly to the study's improvements. They are also thankful for the support of MSU-Marawi, the Mechanical Engineering Department, and all the laboratory and experimental support during the study's data gathering.

References

[1] Sascha Thyer, and Tony White, "Energy Recovery in a Commercial Building Using Pico-Hydropower Turbines: An Australian Case Study," *Heliyon*, vol. 9, no. 6, pp. 1-18, 2023. [CrossRef] [Google Scholar] [Publisher Link]

[2] M.B. Farriz et al., "Evolution of Simple Reaction Type Turbines for Pico-Hydro Applications," *Technology Journal*, vol. 77, no. 32, pp. 1-9, 2015. [CrossRef] [Google Scholar] [Publisher Link]

[3] Ieda Geriberto Hidalgo et al., "Hydropower Generation in Future Climate Scenarios," *Energy for Sustainable Development*, vol. 59, pp. 180-188, 2020. [CrossRef] [Google Scholar] [Publisher Link]

[4] M.F. Basar et al., "Economic Analysis on Design of a Simple Hydraulic Reaction Type Turbine for Low-Head Low-Flow Pico Hydro," *International Journal of Innovative Technology and Exploring Engineering (IJITEE)*, vol. 9, no. 2, pp. 3976-3980, 2019. [CrossRef] [Google Scholar] [Publisher Link]

[5] Abhijit Date, Ashwin Date, and Aliakbar Akbarzadeh, "Investigating the Potential for Using a Simple Water Reaction Turbine for Power Production from Low Head Hydro Resources," *Energy Conversion and Management*, vol. 66, pp. 257-270, 2013. [CrossRef] [Google Scholar] [Publisher Link]

[6] Abhijit Date et al., "Examining the Potential of Split Reaction Water Turbine for Ultra-Low Head Hydro Resources," *Procedia Engineering*, vol. 49, pp. 197-204, 2012. [CrossRef] [Google Scholar] [Publisher Link]

[7] Abhijit Date, and Aliakbar Akbarzadeh, "Design and Analysis of a Split Reaction Water Turbine," *Renewable Energy*, vol. 35, no. 9, pp. 1947-1955, 2010. [CrossRef] [Google Scholar] [Publisher Link]

[8] Nurul Ashikin Mohd Rais et al., "Techno-Economic Evaluations: An Innovative of Hydraulic Reaction Turbine for Pico-Hydro Generation System," *Journal of Advanced Research in Fluid Mechanics and Thermal Sciences*, vol. 90, no. 2, pp. 9-19, 2022. [CrossRef] [Google Scholar] [Publisher Link]

[9] Laura Velásquez et al., "Experimental Optimization of the Propeller Turbine Performance Using the Response Surface Methodology," *Sustainability*, vol. 16, no. 19, pp. 1-18, 2024. [CrossRef] [Google Scholar] [Publisher Link]

[10] Chengming Liu et al., "Flow Characteristics Analysis of a 1 GW Hydraulic Turbine at Rated Condition and Overload Operation Condition," *Processes*, vol. 12, no. 2, pp. 1-19, 2024. [CrossRef] [Google Scholar] [Publisher Link]

[11] L. Xue et al., "Effect of the Guide Vane on the Hydraulic Stability of a Low-Head, Large-Discharge Industrial Hydraulic Turbine," *Journal of Applied Fluid Mechanics*, vol. 17, no. 3, pp. 713-725, 2024. [CrossRef] [Google Scholar] [Publisher Link]

[12] Kotaro Takamure et al., "Effect of Cone on Efficiency Improvement of a Self-Powered IoT-Based Hydro Turbine," *Advances in Mechanical Engineering*, vol. 14, no. 7, pp. 1-9, 2022. [CrossRef] [Google Scholar] [Publisher Link]

[13] Wenlong Tian et al., "Shape Optimization of a Savonius Wind Rotor with Different Convex and Concave Sides," *Renewable Energy*, vol. 117, pp. 287-299, 2018. [CrossRef] [Google Scholar] [Publisher Link]

[14] Surupa Shaw, and Edwin Javier Cortes, "Advanced Flow Control Innovations for Optimizing Wind and Water Turbine Performance: Toward Sustainable Energy Solutions," *Journal of Fluid Flow, Heat and Mass Transfer (JFFHMT)*, vol. 11, no. 1, pp. 404-415, 2024. [CrossRef] [Google Scholar] [Publisher Link]

[15] Jose Bernardes et al., "Hydropower Operation Optimization Using Machine Learning: A Systematic Review," *AI*, vol. 3, no. 1, pp. 78-99, 2022. [CrossRef] [Google Scholar] [Publisher Link]

[16] Guy Richard Wakeley, "*The Optimisation of Steam Turbine Design*," Ph.D. Thesis, Newcastle University, 1997. [Google Scholar] [Publisher Link]

[17] Juan Camilo Pineda, Ainhoa Rubio-Clemente, and Edwin Chica, "Optimization of a Gorlov Helical Turbine for Hydrokinetic Application Using the Response Surface Methodology and Experimental Tests," *Energies*, vol. 17, no. 22, pp. 1-21, 2024. [CrossRef] [Google Scholar] [Publisher Link]

[18] Andrés Chalaca et al., "Design and Optimization of a Gorlov-Type Hydrokinetic Turbine Array for Energy Generation Using Response Surface Methodology," *Energies*, vol. 17, no. 19, pp. 1-21, 2024. [CrossRef] [Google Scholar] [Publisher Link]

[19] Vipin Uniyal, Ashish Karn, and Varun Pratap Singh, "Parametric Optimization of Archimedes Screw Turbine by Response Surface Methodology and Artificial Neural Networks," *Renewable Energy and Sustainable Development*, vol. 10, no. 2, pp. 306-318, 2024. [CrossRef] [Google Scholar] [Publisher Link]

[20] Haymanot Beza Lamesgin, and Addisu Negash Ali, "Optimization of Screw Turbine Design Parameters to Improve the Power Output and Efficiency of Micro-Hydropower Generation," *Cogent Engineering*, vol. 11, no. 1, pp. 1-14, 2024. [CrossRef] [Google Scholar] [Publisher Link]

[21] A.O. Onokwai et al., "Application of Response Surface Methodology (RSM) for the Optimization of Energy Generation from Jebba Hydro-Power Plant, Nigeria," *ISH Journal of Hydraulic Engineering*, vol. 28, no. 1, pp. 1-9, 2022. [CrossRef] [Google Scholar] [Publisher Link]

[22] Sagheer Abbas et al., "Modeling, Simulation and Optimization of Power Plant Energy Sustainability for IoT Enabled Smart Cities Empowered with Deep Extreme Learning Machine," *IEEE Access*, vol. 8, pp. 39982-39997, 2020. [CrossRef] [Google Scholar] [Publisher Link]

[23] Juliana Guerra et al., "Design and Optimization of a Siphon Turbine Using the Response Surface Methodology," *Results in Engineering*, vol. 22, pp. 1-13, 2024. [CrossRef] [Google Scholar] [Publisher Link]

[24] Mahmoud Alidadi, and Sander Calisal, "A Numerical Method for Calculation of Power Output from Ducted Vertical Axis Hydro-Current Turbines," *Computers & Fluids*, vol. 105, pp. 76-81, 2014. [CrossRef] [Google Scholar] [Publisher Link]

[25] Akintayo Temiloluwa Abolude, and Wen Zhou, "Assessment and Performance Evaluation of a Wind Turbine Power Output," *Energies*, vol. 11, no. 8, pp. 1-15, 2018. [CrossRef] [Google Scholar] [Publisher Link]

[26] A.H. Elbatran et al., "Hydro Power and Turbine Systems Reviews," *Technology Journal*, vol. 74, no. 5, pp. 83-90, 2015. [CrossRef] [Google Scholar] [Publisher Link]

[27] Javad Taghinezhad et al., "Performance Optimization of a Dual-Rotor Ducted Wind Turbine by Using Response Surface Method," *Energy Conversion and Management: X*, vol. 12, pp. 1-13, 2021. [CrossRef] [Google Scholar] [Publisher Link]

[28] Avita Ayu Permanasari et al., "Experimental Investigation and Optimization of Floating Blade Water Wheel Turbine Performance Using Taguchi Method and Analysis of Variance (ANOVA)," *IOP Conference Series: Materials Science and Engineering*, vol. 515, pp. 1-11, 2019. [CrossRef] [Google Scholar] [Publisher Link]

[29] Moumtez Bensouici, Mohamed Walid Azizi, and Fatima Zohra Bensouici, "Performance Analysis and Optimization of Regenerative Gas Turbine Power Plant using RSM," *International Journal of Automotive and Mechanical Engineering*, vol. 20, no. 3, pp. 10671-10683, 2023. [CrossRef] [Google Scholar] [Publisher Link]

[30] Moona Mohammadi et al., "Analyzing Mathematical and Software Methods for Selecting and Designing Francis Turbine in Hydropower Plants," *Journal of Clean Energy Technologies*, vol. 4, no. 4, pp. 276-283, 2016. [CrossRef] [Google Scholar] [Publisher Link]

[31] Muhammad Shahbaz Aziz et al., "Design and Analysis of In-Pipe Hydro-Turbine for an Optimized Nearly Zero Energy Building," *Sensors*, vol. 21, no. 23, pp. 1-28, 2021. [CrossRef] [Google Scholar] [Publisher Link]

[32] Hassan Pashaei et al., "Experimental Modeling and Optimization of CO_2 Absorption into Piperazine Solutions Using RSM-CCD Methodology," *ACS Omega*, vol. 5, no. 15, pp. 8432-8448, 2020. [CrossRef] [Google Scholar] [Publisher Link]

[33] Yan Wang, Quanlin Dong, and Yulian Zhang, "Meridional Shape Design and the Internal Flow Investigation of Centrifugal Impeller," *Proceedings of the Institution of Mechanical Engineers, Part C: Journal of Mechanical Engineering Science*, vol. 231, no. 23, pp. 4319-4330, 2016. [CrossRef] [Google Scholar] [Publisher Link]

[34] Yun Jia et al., "Experimental Study of the Effect of Splitter Blades on the Performance Characteristics of Francis Turbines," *Energies*, vol. 12, no. 9, pp. 1-16, 2019. [CrossRef] [Google Scholar] [Publisher Link]

[35] Zheqin Yu et al., "Multiple Parameters and Target Optimization of Splitter Blades for Axial Spiral Blade Blood Pump Using Computational Fluid Mechanics, Neural Networks, and Particle Image Velocimetry Experiment," *Science Progress*, vol. 104, no. 3, pp. 1-19, 2021. [CrossRef] [Google Scholar] [Publisher Link]